Iranian (Iranica) Journal of Energy & Environment
Journal Homepage: www.ijee.net
IJEE an official peer review journal of Babol Noshirvani University of Technology, ISSN:2079-2115

Modeling of a Novel Magneto-electro-elastic Energy Harvesting System Subjected to Applied Electric Voltage with Simultaneous Use as an Electrical Actuator System

M. Moory Shirbani[1]*, M. Shishehsaz[2]

[1] *Faculty of Engineering, Shohadaye Hoveizeh Campus of Technology, Shahid Chamran University of Ahvaz, Iran*
[2] *Faculty of Engineering, Shahid Chamran University of Ahvaz, Ahvaz, Iran*

PAPER INFO

Paper history:
Received 28 May 2022
Accepted in revised form 15 January 2023

Keywords:
Beam of energy harvester
Uni-morph
Magneto-electro-elastic layer
Dual-usage
Actuator-harvester

ABSTRACT

This paper introduces a novel harvester to store the electrical power, which comes from the power of external applied electrical voltage. In the last decade, most of the energy harvesters have been designed and analyzed in the form of cantilever beams. In the present article, the harvesters are analyzed as a cantilever beam with the Euler-Bernoulli beam assumptions. The beam of energy harvester consists of an active Magneto-electro-elastic (MEE) layer attached to the piezoelectric layer. Assuming that the connection of these layers is perfect, the uni-morph configuration is investigated. The magneto-electro-elastic governing coupled equations of the MEE energy harvester are derived for a harmonic external applied electrical voltage in the transversal direction based on Euler-Bernoulli theory, Gaussian law, and Faraday law. These equations are solved analytically to find out the amount of harvested power and voltage. The obtained results state that by adjusting the electromechanical parameters, up to 66% of the input power and 27% of the applied voltage can be harvested. Choosing the right geometric parameters can increase the harvested power and voltages connected to the electrodes and external coil by 120.31%, 49.05% and 60.98%, respectively. Finally, the results prove the usefulness and efficiency of the dual-usage (actuator-harvester) of the new energy harvester.

***doi**: 10.5829/ijee.2023.14.02.09*

NOMENCLATURE

B_i	Components of magnetic flux (Wb/m^2)	z	Direction along thickness of beam
C_{ij}	Elastic stiffness tensor (N/m^2)	**Greek Symbols**	
D_i	Components of electric displacement(C·m^{-2})	η	Normalized natural frequency(-)
E_i	Components of electric field(V/m)	μ_{ij}	Magnetic permittivity constants(N/A^2)
H_i	Components of magnetic field(A/m)	υ_r^{EM}	Mechanical to magnetic modal coupling term(V.s/A)
L	Length of MEE microbeam(m)	ω_r	Natural frequency(rad/s)
M	Bending moment(N.m)	σ_{ij}	Components of stress(N/m^2)
w	Transverse displacement(m)	θ_{EM}	Magneto- mechanical coupled term(N.m/V)
Subscripts		Λ_{ME}	Ratio of harvested to the input power(W/W)
x	Direction along length of beam		

INTRODUCTION

Electrical energy is a valuable type of energy because of its ease of use and efficiency. Today, fossil fuels are the primary energy sources to produce electrical energy. Therefore, the optimal use of these resources is a desirable task because they are a non-recyclable source of energy and have a role in the pollution of the

*Corresponding Author Email: m.mooryshirbani@scu.ac.ir
(M. Moory Shirbani)

Please cite this article as: M. Moory Shirbani, M. Shishehsaz, 2023. Modeling of a Novel Magneto-electro-elastic Energy Harvesting System Subjected to Applied Electric Voltage with Simultaneous Use as an Electrical Actuator System, Iranian (Iranica) Journal of Energy and Environment, 14(2), pp. 168-176. Doi: 10.5829/ijee.2023.14.02.09

environment [1]. Recently, use of wasted energy has become an option to produce electrical energy [2, 3]. This was led to energy harvesting technology. The electrical power produced by this promising technology is usually recyclable and contributes to the sustainability of the system's infrastructure. It is usable in cooling and heating, electricity generation, and health monitoring structures.

One of the most common energy sources for energy harvesting systems is ambient vibrations, which have high energy capacity and are suitable for small-scale devices. The kinetic energy is converted into electricity in three different ways: active materials (such as piezoelectric [4]), electromechanical coupling mechanisms (such as electrostatic [5], and electromagnetism [6]), and the use of special instruments and materials that combine the above [7].

The basis of the work of electrostatic generators is capacitors with variable capacitance. Unfortunately, these generators require an initial polarization voltage or charge. Therefore, they need a battery at the start [5]. A permanent magnet and a coil are used as a converter in electromagnetic generators and work better on the macro-scale [6]. The advantage of these generators is their relatively high output current. The piezoelectric effect is a characteristic of some materials (like material which is called PZT, PVDF, and MFC) that in response to mechanical stresses, the electrical potential created and vice versa. Using each of these three methods to convert the vibration oscillations into electrical power has been separately investigated. The energy harvesting system used one of these methods is called a vibrational energy harvester (VEH).

Using composite and functionally graded, and smart materials attract many researchers due to their special vibrational behaviours [8]. Among them, some smart materials known as MEE composites have received significant interest in material science recently. These materials have both piezoelectric and piezo magnetic properties, and they can convert electrical, magnetic, and mechanical energy into each other. Thus, using MEE composites in energy harvesting systems are recommended [9].

To the best of the author's knowledge, no one was used the energy harvester system under both the electrical excitation and the ambient vibration. One can import an electrical excitation to the energy harvester to amplify the system's vibration and harvest more energy. The results prove that there is an opportunity to save the remaining output voltage in addition to the ambient vibration source of energy.

MODELLING OF AN MEE ENERGY HARVESTER UNDER ELECTRICAL EXCITATION

An electrically excited MEE energy harvester is shown in Figure 1. In this figure, V_{in}, V_E, and V_M represent input voltage, generated voltages on the electrodes attached to the MEE layer and the voltage induced in the N-turn coil, respectively.

A Cartesian coordinate system $(x,y,z)=(x_1,x_2,x_3)$ is used to derive the governing constitutive equations. The coupled constitutive equations for an anisotropic and three-dimensional linear MEE energy harvester beam may be expressed as follows [10]:

$$\begin{aligned} \sigma_i^M &= C_{ik}^M \varepsilon_k^M - e_{ik}^M E_k^M - f_{ik}^M H_k^M \\ D_i^M &= e_{ik}^M \varepsilon_k^M + h_{ik}^M E_k^M - g_{ik}^M H_k^M \qquad \begin{matrix} i = 1,2,\ldots,6 \\ k = 1,2,3 \end{matrix} \\ B_i^M &= f_{ik}^M \varepsilon_k^M + g_{ik}^M E_k^M + \mu_{ik}^M H_k^M \end{aligned} \tag{1}$$

where σ_i, D_i and B_i are the stress, electric displacement, and magnetic induction (i.e., magnetic flux); ε_i, E_i and H_i are the strain, electric and magnetic fields; C_{ij}, h_{ij}, and μ_{ij} are the elastic, dielectric, and magnetic permeability coefficients; e_{ij}, f_{ij} and g_{ij} are the piezoelectric, piezomagnetic and magnetoelectric coefficients, respectively. The standard contraction indices have been used for the elastic variables (i.e., $\varepsilon_4 = \varepsilon_{23}$, etc.).

Because the thickness of the beam is significantly less than its radius of curvature under different loads, the in-plane electric and magnetic fields can be ignored (i.e., $E_1 = E_2 = 0$ and $H_1 = H_2 = 0$). So, the coupled constitutive Equations (1) reduced into Equations (2). and the analytical equations are derived using Euler-Bernoulli beam theory [10].

$$\sigma_1^M = C_{11}^M \varepsilon_1^M - e_{31}^M E_3^M - f_{31}^M H_3^M \tag{2a}$$

$$D_3^M = e_{31}^M \varepsilon_1^M + h_{33}^M E_3^M - g_{33}^M H_3^M \tag{2b}$$

$$B_3^M = f_{31}^M \varepsilon_1^M + g_{33}^M E_3^M + \mu_{33}^M H_3^M \tag{2c}$$

The constitutive equation of the piezoelectric layer is as follows [10]:

$$\sigma_1^p = C_{11}^p \varepsilon_1^p - e_{31}^p E_3^p \tag{3}$$

Assuming the electric field is uniform throughout the constant piezoelectric layer thickness h_p, then the electric field E_3^P, exist in terms of the input voltage V_{in} (connected to the resistive loads R_{in}) across the thickness of the

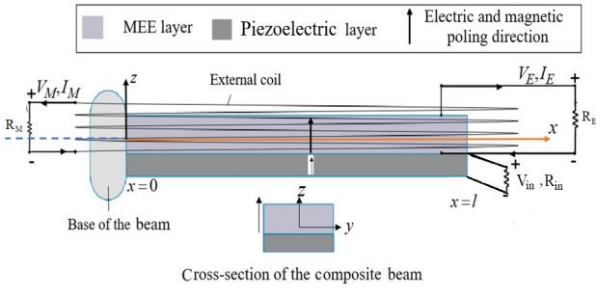

Figure 1. The MEE energy harvester under the electrical excitation

piezoelectric layer. Also, the electrical field of the MEE layer E_3^M, in terms of the voltage V_E can be expressed as follows [8]:

$$E_3{}^p(t) = -\frac{V_{in}(t)}{h_p} \quad (4a)$$

$$E_3{}^M(t) = -\frac{V_E(t)}{h_M} \quad (4b)$$

With the help of Faraday's law, the magnetic field $H_3(t)$ can be obtained in terms of the current $i_M(t)$ and the number of turns of the coil N as expressed in the following relation [11].

$$H_3(t) = \frac{Ni_M(t)}{h_M} \overset{i_M=\frac{V_M}{R_M}}{=} \frac{NV_M(t)}{R_M h_M} \quad (5)$$

The basic equations listed will be used to derive the coupled magneto-electro-elastic equations from investigating the performance of a MEE energy harvester.

The relative deflection of the neutral axis, $w(x,t)$, is caused by electrical excitation, V_{in}. The following equation is the governing equation of vibration of the beam under base excitation [12]:

$$M_{,xx} + c_k I \dot{w}_{,xxxx} + c_m \dot{w} + m\ddot{w} = 0 \quad (6)$$

where I is the moment of the cross section of the beam, c_m viscous air damping coefficient, c_kI equivalent composite structural damping coefficient, and m is the mass per unit length of the beam. Also, $M(x,t)$ is the internal bending moment of the beam which is calculated for Uni-morph configuration of the MEE energy harvester by Equation (7) .

$$M(x,t) = -b\left(\int_{h_b}^{h_c} \sigma_1^M z dz + \int_{h_a}^{h_b} \sigma_1^p z dz\right) \quad (7a)$$

where b is the width of the beam, h_a, h_b, h_c, h_M, and h_p, are defined in Figure 2, and $\bar{z}$ is the location of the neutral axis.

Substituting Equations (2) and Equation (3) into Equations (7), the internal bending moment for each configuration is obtained as follows [12]:

$$\begin{aligned} M(x,t) = & \underbrace{CI\frac{\partial^2 w(x,t)}{\partial x^2}}_{M_{Elas}(x,t)} + \\ & \underbrace{\Theta_{EM}V_E(t)[H(x)-H(x-L)]}_{M_{Elec}(x,t)} + \\ & \underbrace{\Theta_{MM}V_M(t)[H(x)-H(x-L)]}_{M_{Mag}(x,t)} + \underbrace{\Theta_{in}V_{in}(t)}_{M_{in}(x,t)}[H(x) - \\ & H(x-L)] \end{aligned} \quad (8)$$

where Θ_{in}, Θ_{EM} and Θ_{MM} are the electro- and magneto-mechancial coupled terms and defined as follows:

$$\Theta_{in} = \frac{be_{31}^p}{2h_p}[(h_b)^2 - (h_a)^2] \quad (9a)$$

$$\Theta_{EM} = \frac{be_{31}^M}{2h_M}[(h_c)^2 - (h_b)^2] \quad (9b)$$

$$\Theta_{MM} = -\frac{bf_{31}^M}{2h_M}\frac{N}{R_M}[(h_c)^2 - (h_b)^2] \quad (9c)$$

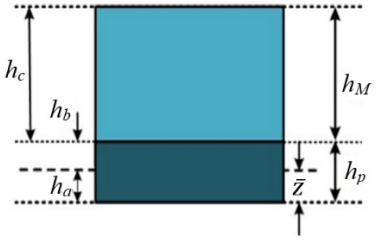

Figure 2. The cross-section area of the Unimorph configuration MEE energy harvester

Also, the equivalent composite structural damping coefficient (CI) and mass per unit length of the beam (m) are defined by Equations (10) :

$$CI = \frac{C_{11}^p b}{3}[(h_b)^3 - (h_a)^3] + \frac{C_{11}^M b}{3}[(h_c)^3 - (h_b)^3] \quad (10a)$$

$$m = b(\rho_M h_M + \rho_p h_p) \quad (10b)$$

where ρ_m and ρ_p are the density of MEE and piezoelectric layers, respectively.

By substituting Equations (8-10) into Equation (6), the governing differential equation of the harvester beam for each configuration is achieved.

$$\begin{aligned} & CI\frac{\partial^4 w\ (x,t)}{\partial x^4} + \Theta_{EM}V_E(t)\left[\frac{d\delta(x)}{dx} - \frac{d\delta(x-L)}{dx}\right] + \\ & \Theta_{MM}V_M(t)\left[\frac{d\delta(x)}{dx} - \frac{d\delta(x-L)}{dx}\right] + \\ & \Theta_{in}V_{in}(t)\left[\frac{d\delta(x)}{dx} - \frac{d\delta(x-L)}{dx}\right]c_k I\frac{\partial^5 w\ (x,t)}{\partial x^4 \partial t} + \\ & c_m\frac{\partial w\ (x,t)}{\partial t} + m\frac{\partial^2 w\ (x,t)}{\partial t^2} = 0 \end{aligned} \quad (11)$$

Using the separation of variables method, one can write the relative deflection as follows [13]:

$$w(x,t) = \sum_{r=0}^{\infty} W_r(x)T_r(t) \quad (12)$$

where $T_r(t)$ and $W_r(x)$ are the time response and the r-th normal mode shape of the cantilever beam, respectively. Then, the motion equation in modal space can be written as Equation (12).

$$\begin{aligned} & \frac{d^2T_r(t)}{dt^2} + 2\zeta_r\omega_r\frac{dT_r(t)}{dt} + \omega_r^2 T_r(t) + \alpha_{EMr}V_E(t) + \\ & \alpha_{MMr}V_M(t) = FV_{in,r}(t) \end{aligned} \quad (13)$$

where $FV_{in,r}(t)$ is the electrical excitation induced force and expressed as follows:

$$FV_{in,r}(t) = -\alpha_{in}V_{in}(t) \quad (14a)$$

where;

$$\begin{aligned} \alpha_{inr} &= \frac{be_{31}^p}{2h_p}[(h_b)^2 - (h_a)^2]\frac{dW_r(x)}{dx}\Big|_{x=L} \\ \alpha_{EMr} &= \frac{be_{31}^M}{2h_M}[(h_c)^2 - (h_b)^2]\frac{dW_r(x)}{dx}\Big|_{x=L} \\ \alpha_{MMr} &= -\frac{bf_{31}^M}{2h_M}\frac{N}{R_M}[(h_c)^2 - (h_b)^2]\frac{dW_r(x)}{dx}\Big|_{x=L} \end{aligned} \quad (14b)$$

Now, the differential equation of the electrical circuit of the two ends of the electrodes used around the MEE

layers is extracted. Initially, the two ends of the electrodes and external coils were connected to external electrical resistors R_E and R_M to use the voltages generated by V_E and V_M.

Using Equation (4), the second constitutive Equation (2b), is reduced to Equation (15) for the MEE energy harvester.

$$D_3^M(x,t) = -e_{31}^M h_{Mc} \frac{\partial^2 w\ (x,t)}{\partial x^2} - \frac{h_{33}^M}{h_M} V_E(t) + \frac{g_{33}^M N}{R_M h_M} V_M(t) \quad (15)$$

where h_{Mc} is the distance between the neutral and mid axes of the active MEE and sgn(z) is the sign function.

Next, integrating the electric displacement in Equation (14) over the surface of the electrodes, using Gauss's law, the electrical charge $Q_E(t)$ appearing on the electrode attached to the MEE layer can be expressed as follows [12]:

$$Q_E(t) = \iint_{A_e} D_3^M(x,t) dA_e\ dA_e = dxdy \quad (16)$$

By imposing Equation (15) into Equation (16), for each configuration, and calculating the integral, an expression for the charge is obtained as a function of time.

$$C_M \frac{dV_E(t)}{dt} + \frac{1}{R_E} V_E(t) = \sum_{r=1}^{\infty} \vartheta_{MEr} \frac{dT_r(t)}{dt} + \chi_{ME} \frac{dV_M(t)}{dt} \quad (17)$$

C_M denotes the internal capacitance of the MEE layer, and ϑ_r^{EM} and χ_{ME} are the coefficients of modal and magnetic to electric coupling terms in the circuit connected to the electrodes, respectively. That are obtained in the following forms:

$$C_M = \frac{h_{33}^M bL}{h_M} \quad (18a)$$

$$\vartheta_{MEr} = -e_{31}^M h_{Mc} b \frac{dW_r(x)}{dx}\Big|_{x=L} \quad (18b)$$

$$\chi_{ME} = \frac{g_{33}^M N}{R_M} \frac{bL}{h_M} \quad (18c)$$

One can rewrite Equations (17) into general form as Equation (19).

$$C_M \frac{dV_E(t)}{dt} + \frac{1}{R_E} V_E(t) = \sum_{r=1}^{\infty} \vartheta_{MEr} \frac{dT_r(t)}{dt} + \chi_{ME} \frac{dV_M(t)}{dt} \quad (19)$$

Faraday's law states that the voltage V is induced proportional to the time derivative of magnetic flux linkage, ϕ, [14]. As a result, the voltage induced in the N-turn coil V_M may be calculated as follows:

$$V_M(t) = -N \frac{d\phi}{dt} \quad (20)$$

Generally, ϕ, is calculated as follows:

$$\phi = \sum_{i=1}^{N} \int_{A_i} B.dA \quad (21)$$

According to substitution of Equation (5) into Equation (2c) and using Table 2, the magnetic field flux density, B_3^M, is obtained as:

$$B_3^M(x,t) = -f_{31}^M h_{Mc} \frac{\partial^2 w\ (x,t)}{\partial x^2} - \frac{g_{33}^M}{h_M} V_E(t) + \frac{\mu_{33}^M N}{R_M h_M} V_M(t) \quad (22)$$

Using Equations (20), (21), and (22), the below differential equations are obtained as follows:

$$L_c \frac{dV_M(t)}{dt} + R_M V_M(t) = \sum_{r=1}^{\infty} \vartheta_{MMr} \frac{dT_r(t)}{dt} + \chi_{EM} \frac{dV_E(t)}{dt} \quad (23)$$

Here, L_c, ϑ_r^{MM}, and χ_{EM} represent self-inductance of the coil, the coefficient of modal and electric to magnetic coupling terms, respectively. That are obtained in the following forms:

$$L_c = \mu_{33}^M N^2 \frac{bl}{h_M} \quad (24a)$$

$$\vartheta_{MMr} = -f_{31}^M N R_M b h_{Mc} \frac{dW_r(x)}{dx}\Big|_{x=L} \quad (24b)$$

$$\chi_{EM} = g_{33}^M N R_M \frac{bl}{h_M} \quad (24c)$$

One can reduce Equations (24) into general form as follows:

$$L_c \frac{dV_M(t)}{dt} + R_M V_M(t) = \sum_{r=1}^{\infty} \vartheta_{MMr} \frac{dT_r(t)}{dt} + \chi_{EM} \frac{dV_E(t)}{dt} \quad (25)$$

Finally, the governing differential equations of the electrically excited MEE energy harvester are classified as follows:

$$\begin{aligned} &\frac{d^2T_r(t)}{dt^2} + 2\zeta_r\omega_r \frac{dT_r(t)}{dt} + \omega_r^2 T_r(t) + \alpha_{EMr} V_E(t) + \\ &\alpha_{MMr} V_M(t) = FV_{in,r}(t)\ C_M \frac{dV_E(t)}{dt} + \frac{1}{R_E} V_E(t) = \\ &\sum_{r=1}^{\infty} \vartheta_{MEr} \frac{dT_r(t)}{dt} + \chi_{ME} \frac{dV_M(t)}{dt}\ L_c \frac{dV_M(t)}{dt} + \\ &R_M V_M(t) = \sum_{r=1}^{\infty} \vartheta_{MMr} \frac{dT_r(t)}{dt} + \chi_{EM} \frac{dV_E(t)}{dt} \end{aligned} \quad (26)$$

Next, in order to derive analytical expressions for the dynamic response of the MEE energy harvester, it is assumed that the applied voltage, $V_{in}(t)$, is defined as $V_{in}(t) = V_{Ain} e^{j\omega t}$ (where V_{Ain} is the amplitude of the applied voltage). Similarly, the time response expression of the beam in modal space (Equation (12)), $T_r(t)$, and the generated voltages, $V_E(t)$ and $V_M(t)$, can be expressed as follows:

$$V_E(t) = V_{AE} e^{j\omega t} \quad (27a)$$

$$V_M(t) = V_{AM} e^{j\omega t} \quad (27b)$$

$$T_r(t) = T_{Ar} e^{j\omega t} \quad (27c)$$

where T_{Ar}, V_{AE} and V_{AM} are the temporal response and generated voltage amplitudes, respectively. Thus, one

can rewrite the electrical excitation induced force (Equation (14)) as follows:

$$FV_{in,r}(t) = FV_{Ar}e^{j\omega t} \tag{28}$$

where;

$$FV_{Ar} = -\alpha_{EMr}V_{Ain}$$

Substituting Equations (27) and (28) into Equation (26):

$$\begin{matrix}[(\omega_r{}^2 - \omega^2) + j(2\zeta_r\omega_r\omega)]T_{Ar} + \alpha_{EMr}V_{AE} + \\ \alpha_{MMr}V_{AM} = FV_{Ar}\,(\frac{1}{R_E} + j\omega C_M)V_{AE} = \\ j\omega[\sum_{r=1}^{\infty}\vartheta_{MEr}T_{Ar} + \chi_{ME}V_{AM}] \quad (R_M + j\omega L_c)V_{AM} = \\ j\omega[\sum_{r=1}^{\infty}\vartheta_{MMr}T_{Ar} + \chi_{EM}V_{AE}]\end{matrix} \tag{29}$$

By solving the Equation (29) and substituting the results in Equation (27):

$$V_E(t) = \frac{\sum_{r=1}^{\infty}\frac{j\omega\vartheta_{MEr}FV_{Ar}}{[(\omega_r{}^2-\omega^2)+j(2\zeta_r\omega_r\omega)]}e^{j\omega t}}{\left[(\frac{1}{R_E}+j\omega C_M)+\sum_{r=1}^{\infty}\frac{j\omega\vartheta_{MEr}\alpha_{EMr}}{[(\omega_r{}^2-\omega^2)+j(2\zeta_r\omega_r\omega)]}\right]+ n_{ME}\left[\sum_{r=1}^{\infty}\frac{j\omega\vartheta_{MEr}\alpha_{MMr}}{[(\omega_r{}^2-\omega^2)+j(2\zeta_r\omega_r\omega)]}-\chi_{ME}\right]} \tag{30a}$$

$$V_M(t) = \frac{\sum_{r=1}^{\infty}\frac{j\omega\vartheta_{MMr}FV_{Ar}}{[(\omega_r{}^2-\omega^2)+j(2\zeta_r\omega_r\omega)]}e^{j\omega t}}{\left[(R_M+j\omega L_c)+\sum_{r=1}^{\infty}\frac{j\omega\vartheta_{MMr}\alpha_{MMr}}{[(\omega_r{}^2-\omega^2)+j(2\zeta_r\omega_r\omega)]}\right]+ n_{EM}\left[\sum_{r=1}^{\infty}\frac{j\omega\vartheta_{MMr}\alpha_{EMr}}{[(\omega_r{}^2-\omega^2)+j(2\zeta_r\omega_r\omega)]}-\chi_{EM}\right]} \tag{30b}$$

$$T_r(t) = \begin{bmatrix} 1 - \frac{\sum_{r=1}^{\infty}\frac{j\omega\vartheta_{MEr}\alpha_{EMr}FV_{Ar}e^{j\omega t}}{[(\omega_r{}^2-\omega^2)+j(2\zeta_r\omega_r\omega)]^2}}{\left[(\frac{1}{R_E}+j\omega C_M)+\sum_{r=1}^{\infty}\frac{j\omega\vartheta_{MEr}\alpha_{EMr}}{[(\omega_r{}^2-\omega^2)+j(2\zeta_r\omega_r\omega)]}\right]+ n_{ME}\left[\sum_{r=1}^{\infty}\frac{j\omega\vartheta_{MEr}\alpha_{MMr}}{[(\omega_r{}^2-\omega^2)+j(2\zeta_r\omega_r\omega)]}-\chi_{ME}\right]} \\ - \frac{\sum_{r=1}^{\infty}\frac{j\omega\vartheta_{MMr}\alpha_{MMr}FV_{Ar}e^{j\omega t}}{[(\omega_r{}^2-\omega^2)+j(2\zeta_r\omega_r\omega)]^2}}{\left[(R_M+j\omega L_c)+\sum_{r=1}^{\infty}\frac{j\omega\vartheta_{MMr}\alpha_{MMr}}{[(\omega_r{}^2-\omega^2)+j(2\zeta_r\omega_r\omega)]}\right]+ n_{EM}\left[\sum_{r=1}^{\infty}\frac{j\omega\vartheta_{MMr}\alpha_{EMr}}{[(\omega_r{}^2-\omega^2)+j(2\zeta_r\omega_r\omega)]}-\chi_{EM}\right]} \end{bmatrix} \tag{31}$$

where electromagnetic voltage ratio, V_{ME}, is obtained as follows:

$$n_{ME} = \frac{1}{n_{EM}} = \frac{V_M}{V_E} = \frac{\left[f_{31}^M N R_M(\frac{1}{R_E}+j\omega C_M) - j\omega(e_{31}^M\chi_{EM})\right]}{\left[j\omega(f_{31}^M N R_M\chi_{ME}) - e_{31}^M(R_M+j\omega L_c)\right]} \tag{32}$$

Substituting Equation (31) into Equation (12), the displacement of each point on the MEE energy harvester under electrical excitation is obtained. The electric current frequency response functions are obtained by dividing the resulting voltages by the load resistance of the electrical circuits.

In order to compute the MEE energy harvester efficiency under electrical excitations, the input and output power must be compared. Thus, using Ohm's law ($V = iR$), and $P = 0.5Vi$, the total power made by energy harvester , $P_{total}(t)$, are expressed as follows:

$$P_E(t) = \frac{1}{2R_E}(V_E)^2 \tag{33a}$$

$$P_M(t) = \frac{1}{2R_M}(V_M)^2 \tag{33a}$$

$$P_{total}(t) = P_E(t) + P_M(t) \tag{33b}$$

The MEE energy harvester efficiencies under electric excitation, Λ_E, Λ_M and Λ_{ME}, are introduced as the ratio of harvested to the input parameters and expressed as follows:

$$\Lambda_E = \frac{V_E(t)}{V_{in}(t)} \tag{34a}$$

$$\Lambda_M = \frac{V_E(t)}{V_{in}(t)} \tag{34b}$$

$$\Lambda_{ME} = \frac{P_{total}(t)}{P_{in}(t)} \tag{34c}$$

RESULTS AND DISCUSSION

In this section, the results obtained from the analytical solutions in the previous section are presented. Numerical results will be carried out for *BaTiO3-CoFe$_2$O$_4$* composite as the MEE layer with a volume fraction$v_f = 0.5$. The geometry and material properties used in the following case studies are listed in Table 1.

The performance of the MEE energy harvesting system under external electrical excitation is considered. The effect of the parameters extracted from the previous section, R_M, R_E, R_{in}, h_p and h_M on the MEE energy harvester efficiencies, Λ_E, Λ_M and Λ_{ME} has been investigated.

The effects of the non-dimensional electrical excitation frequency, η, on the power efficiency, Λ_{ME}, for four different values of the electrical load resistances connected to the applied circuit voltage (R_{in} = $10^6\Omega$,

Table 1. Material properties and geometric dimensions of the layers of the harvester

Item		Value
C_{11}^p *(N m^{-2})*	Piezoelectric Young's modulus	117×10^9
C_{11}^M *(N m^{-2})*	MEE material Young's modulus	215×10^9
e_{31}^p *(C m^{-2})*	Piezoelectric coefficient of the Piezoelectric layer	-6.5
e_{31}^M *(C m^{-2})*	Piezoelectric coefficient of the MEE layer	-2.8
f_{31} *(N A^{-1})*	Piezomagnetic coefficient	220
h_{33} *(C^2 N^{-1} m^{-2})*	Dielectric coefficient	6.3×10^{-9}
g_{33} *(N s V^{-1} C^{-1})*	Magnetoelectric coefficient	2750×10^{-12}
μ_{33} *(N s^2 C^{-2})*	Magnetic permeability	83.5×10^{-6}
ρ_p *(kg m^{-3})*	Piezoelectric density	7500
ρ_M *(kg m^{-3})*	MEE material density	5550
l *(mm)*	Length of the beam	80
b *(mm)*	Width of the beam	16
h_p *(mm)*	Thickness of the piezoelectric layer	0.5
h_M *(mm)*	Thickness of the MEE layer	0.5

$10^{5.5}\Omega$, $10^{5}\Omega$, and $10^{4}\Omega$) are plotted in Figure 3. It is evident that an increase in η and R_{in}, leads to an increase in the Λ_{ME}. Figure 3 shows that the maximum value of Λ_{ME} is calculated for $R_{in} = 10^{6}\Omega$ (Λ_{ME} = 0.4758 *W/W*). In other words, 47.58% of the input power can be stored. While this ratio is only equal to 0.51% for the amount of $R_{in} = 10^{4}\Omega$. Due to the fact that electrical load resistance R_{in}, has no effect on the values of voltage efficiency, only its effect on the power efficiency has been investigated.

In Figures 4 to 6 the effects of the η and R_E, on the Λ_{ME}, Λ_E and Λ_M for four different values of the electrical load resistances connected to the electrical circuit of the electrodes (R_E = $10^{6}\Omega$, $10^{5.5}\Omega$, $10^{5}\Omega$, and $10^{4}\Omega$) are plotted. The plotted results show the different effect of each value of electrical resistance R_E in increasing or decreasing efficiencies. From the drawn results, it can be concluded that in order to harvest the maximum power, the range $10^{5}\Omega \leq R_E \leq 10^{5.5}\Omega$ should have a higher priority in the choice of R_E. It is obvious from Figure 5 that for $R_E = 10^{6}\Omega$, 26.87% of the applied voltage can be stored in the circuit connected to the electrodes, which is a significant amount to reduce the consumption of electronic circuits. In order to store higher voltage values, the range $10^{5.5}\Omega \leq R_E \leq 10^{6}\Omega$ must be selected. Also, the maximum efficiency Λ_M occur in $R_E = 10^{5}\Omega$ to the numerical value of Λ_M= *0.0014 V/V* that is insignificant compared to the Λ_E.

Figures 7 to 9 illustrate the effects of the η and R_M, on the Λ_{ME}, Λ_E and Λ_M for four different values of the electrical load resistances connected to the electrical circuit of the external coil (R_M = $10^{6}\Omega$, $10^{4}\Omega$, $10^{2}\Omega$, and $10^{1}\Omega$). The results show the better performance of the MEE harvester in the range of $10^{1}\Omega \leq R_M \leq 10^{2}\Omega$ for

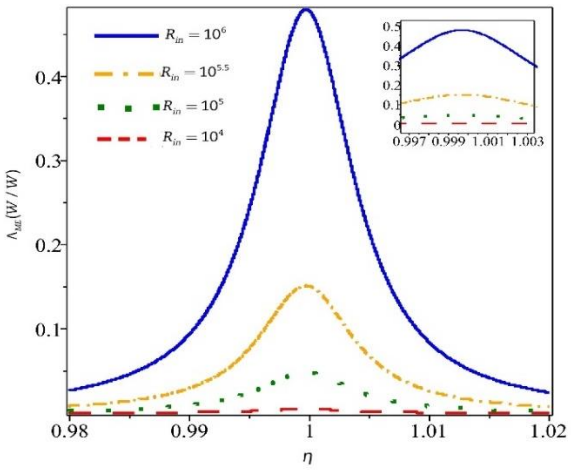

Figure 3. Frequency response curves of the harvested power ratio Λ_{ME} , of the unimorph MEE beam around the first natural frequency for different values of R_{in}

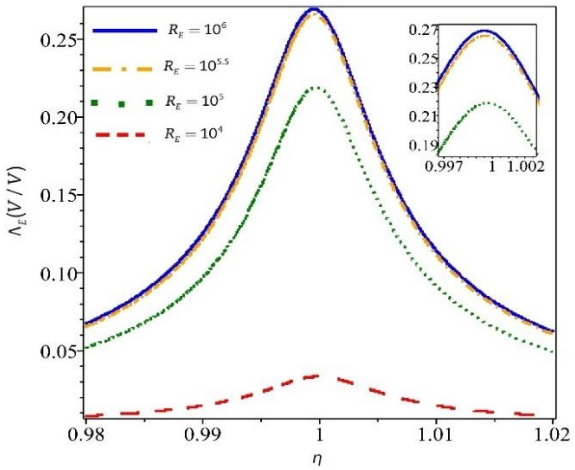

Figure 5. Frequency response curves of the generated voltage over electrodes ratio Λ_E, of the unimorph MEE beam around the first natural frequency for different values of R_E

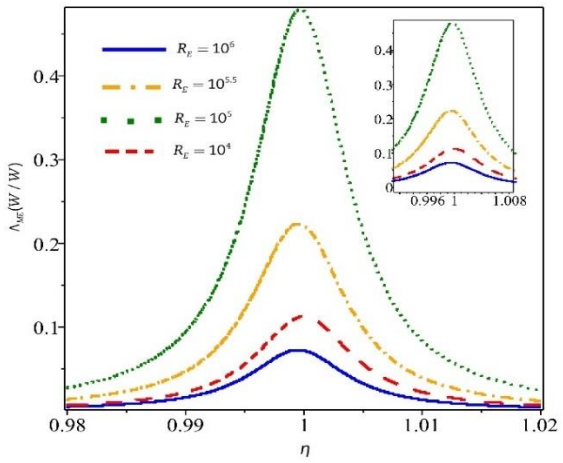

Figure 4. Frequency response curves of the harvested power ratio Λ_{ME}, of the unimorph MEE beam around the first natural frequency for different values of R_E

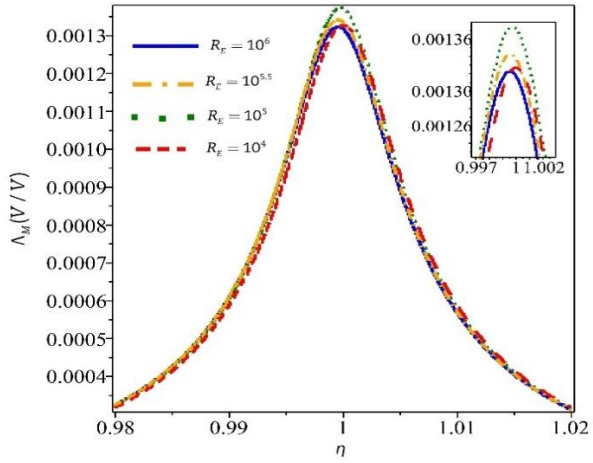

Figure 6. Frequency response curves of the generated voltage over external coil ratio Λ_M, of the unimorph MEE beam around the first natural frequency for different values of R_E

harvesting electric power. The maximum value of Λ_{ME} is calculated for $R_M = 10^1\Omega$ (Λ_{ME} = 0.6596 W/W) that this value is 36.78% better than the value obtained from the results of Figure 4. As a result, the load resistance R_M connected to the external coil can have a decisive role on the power efficiency Λ_{ME}. It can be seen that electrical resistance R_M has little effect on changes in electrical voltage efficiencies. The changes of R_M improve the values of Λ_E and Λ_M by 15.98% and 6.21%, respectively.

Finally by considering that the thickness of harvesters is the limiting parameter of the design, harvester efficiencies Λ_{ME} , Λ_E and Λ_M were checked for different thickness ratios in Figures 10 to 12, respectively. The obtained results show that the equal thickness of the piezoelectric and MEE layers has a better effect on the power and voltage efficiencies of the discussed harvester.

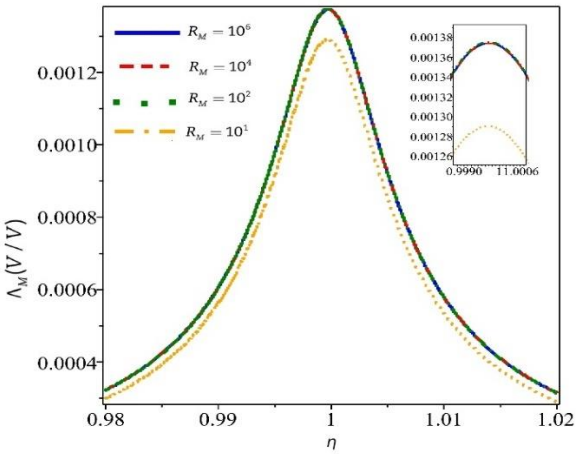

Figure 9. Frequency response curves of the generated voltage over external coil ratio Λ_M, of the unimorph MEE beam around the first natural frequency for different values of R_M

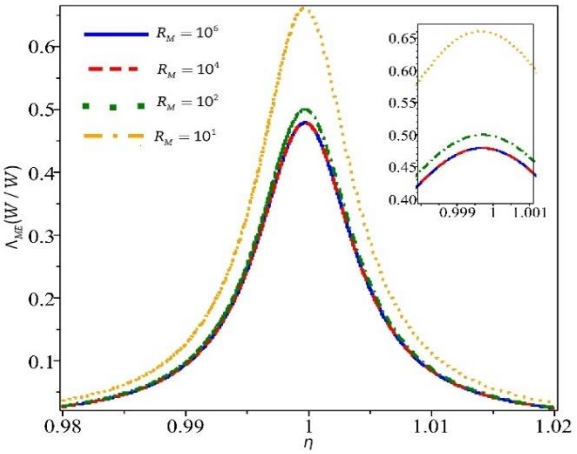

Figure 7. Frequency response curves of the harvested power ratio Λ_{ME}, of the unimorph MEE beam around the first natural frequency for different values of R_M

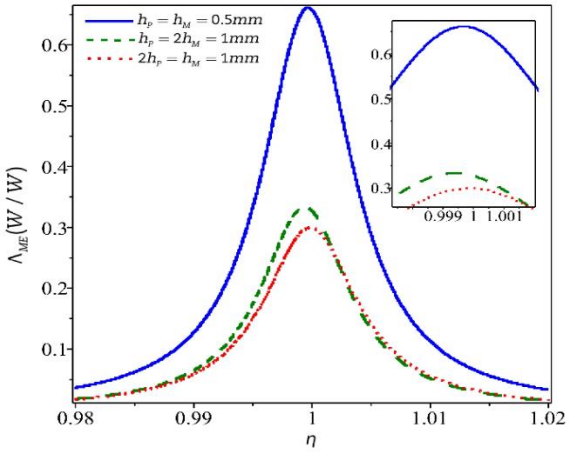

Figure 10. Frequency response curves of the harvested power ratio Λ_{ME}, of the unimorph MEE beam around the first natural frequency for different thickness ratios

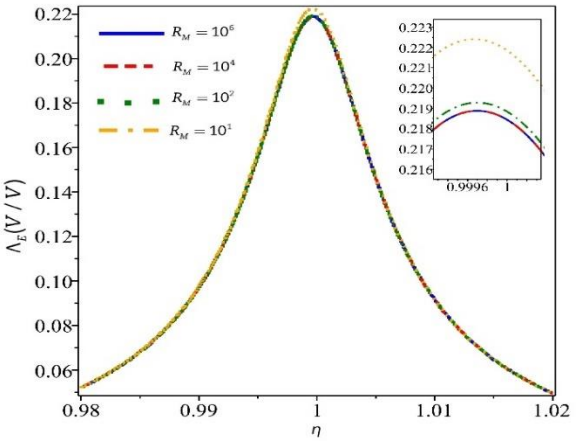

Figure 8. Frequency response curves of the generated voltage over electrodes ratio Λ_E, of the unimorph MEE beam around the first natural frequency for different values of R_M

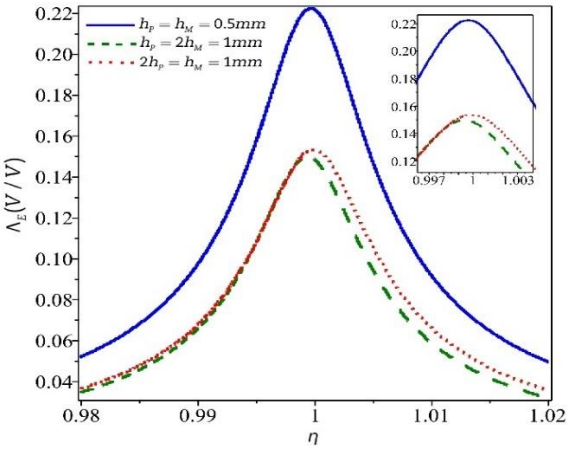

Figure 11. Frequency response curves of the generated voltage over electrodes ratio Λ_E, of the unimorph MEE beam around the first natural frequency for different thickness ratios

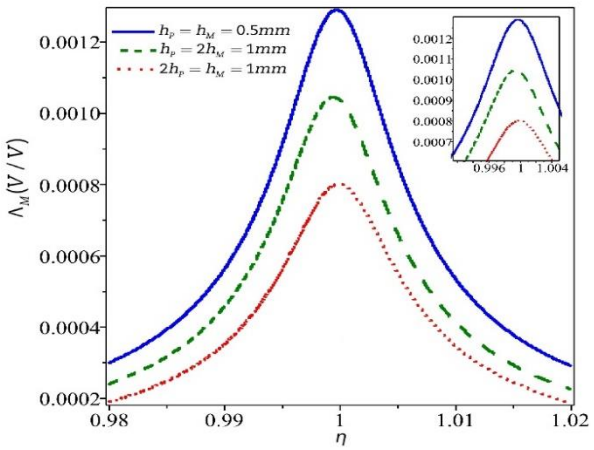

Figure 12. Frequency response curves of the generated voltage over external coil ratio Λ_M, of the unimorph MEE beam around the first natural frequency for different thickness ratios

CONCLUSION

In this paper the performance of the energy harvesters made of active MEE layers and under electrical excitation was analyzed. The MEE beam consisted of the piezoelectric material as the substrate layer and MEE composite as the active layer. The unimorph and bimorph configurations of the MEE layers (including serial, parallel, and single-layer connections) were studied, assuming that the connections between these layers are perfect. The coupled magneto-electro-elastic governing equations were obtained using Euler-Bernoulli theory, Faraday laws and Gauss, and then, these equations were solved analytically to obtain the generated electrical power and voltage. The effects of R_M, R_E, and R_{in}, on the MEE energy harvester efficiencies, have been investigated. The results show that a significant amount of electrical excitation voltage can be stored from the circuits connected to the electrodes. Also, the load resistance R_M connected to the external coil can have a decisive role on the power efficiency. For energy harvesting purposes, one can use the electrical excitation as the second source added to the ambient vibration.

REFERENCES

1. Singh, A. and Singh, K.K., 2022. An Overview of the Environmental and Health Consequences of Air Pollution. *Iranian (Iranica) Journal of Energy & Environment*, 13(3), pp.231-237. Doi: 10.5829/ijee.2022.13.03.03.

2. Esmaeili , S. M. and Hojati, J., 2021. Floating Solar Power Plants: A Way to Improve Environmental and Operational Flexibility. *Iranian (Iranica) Journal of Energy & Environment*, 12(4), pp.337-348. Doi: 10.5829/ijee.2021.12.04.07.

3. Esmaeili , S. M. and Hojati, J., 2021. Floating Solar Power Plants: A Way to Improve Environmental and Operational Flexibility. *Iranian (Iranica) Journal of Energy & Environment*, 12(4), pp.337-348. Doi: 10.5829/ijee.2021.12.04.07.

4. Aghanezhad, M., Shafaghat, R., Alamian, R., Seyedi, S.M.A. and Raji Asadabadi, M.J., 2022. Experimental Study on Performance Assessment of Hydraulic Power Take-off System in Centipede Wave Energy Converter Considering Caspian Sea Wave Characteristics. *International Journal of Engineering*, 35(5), pp.883-899, Doi: 10.5829/ije.2022.35.05b.05.

5. Khan, F.U. and Qadir, M.U. 2016. State-of-the-art in vibration-based electrostatic energy harvesting. *Journal of Micromechanics and Microengineering*, *26*(10), p.103001, Doi: 10.1088/0960-1317/26/10/103001.

6. Reissman, T., Park, J.S. and Garcia, E., 2008. Micro-solenoid electromagnetic power harvesting for vibrating systems. *In Active and Passive Smart Structures and Integrated Systems*, 6928, p. 692806, Doi: 10.1117/12.776493.

7. Yan, Z. 2017. Modeling of a nanoscale flexoelectric energy harvester with surface effects. *Physica E: Low-dimensional Systems and Nanostructures*, *88*, pp.125-132, Doi: 10.1016/j.physe.2017.01.001.

8. Maamer, B., Boughamoura, A., El-Bab, A.M.F., Francis, L.A. and Tounsi, F. 2019. A review on design improvements and techniques for mechanical energy harvesting using piezoelectric and electromagnetic schemes. *Energy Conversion and Management*, 199, p.111973, Doi: 10.1016/j.enconman.2019.111973.

9. Benveniste, Y. 1995. Magnetoelectric effect in fibrous composites with piezoelectric and piezomagnetic phases. *Physical Review B*, 51(22), p.16424, Doi: 10.1103/PhysRevB.51.16424.

10. Chen, Z., Yu, S., Meng, L. and Lin, Y. 2002. Effective properties of layered magneto-electro-elastic composites. *Composite Structures*, *7*(1-4), pp.177-182, Doi: 10.1016/S0263-8223(02)00081-8.

11. Nan, C.W. 1994. Magnetoelectric effect in composites of piezoelectric and piezomagnetic phases. *Physical Review B*, 50(9), p.6082, Doi: 10.1103/PhysRevB.50.6082.

12. Shirbani, M.M., Shishesaz, M., Hajnayeb, A. and Sedighi, H.M., 2017. Coupled magneto-electro-mechanical lumped parameter model for a novel vibration based magneto-electro-elastic energy harvesting systems. *Physica E: Low-dimensional Systems and Nanostructures*, 90, pp.158-169. Doi: 10.1016/j.physe.2017.03.022.

13. Shirbani, M.M., Shishesaz, M., Sedighi, H.M. and Hajnayeb, A., 2017. Parametric modeling of a novel longitudinal vibration-based energy harvester using magneto-electro-elastic materials. *Microsystem Technologies*, *23*(12), pp.5989-6004. Doi: 10.1007/s00542-017-3402-0.

14. Jackson J. D. 1999. "Classical electrodynamics," ed: American Association of Physics Teachers, Doi: 10.1119/1.19136.

Persian Abstract

چکیده

در این مقاله، یک برداشت‌کننده جدید به منظور ذخیره توان الکتریکی که از توان ولتاژ الکتریکی اعمال شده خارجی ناشی می‌شود، معرفی می‌گردد. برداشت‌کننده انرژی به شکل تیر و متشکل از یک لایه با خواص فعال مگنتو-الکترو-الاستیک متصل به یک لایه پیزوالکتریک است. بررسی برداشت‌کننده با فرض اتصال کامل بین لایه‌ها و پیکربندی تک لایه فعال صورت گرفته است. معادلات دیفرانسیل کوپل شده مغناطیسی-الکتریکی-مکانیکی حاکم بر سیستم برداشت‌کننده انرژی مگنتو-الکترو-الاستیک در جهت عرضی و تحت تأثیر یک ولتاژ الکتریکی هارمونیک اعمالی بر اساس نظریه‌های تیر اویلر-برنولی، قانون گاوس و قانون فارادی بدست آمده‌اند. این معادلات به صورت تحلیلی حل شدند تا بتوان میزان توان و ولتاژ برداشت‌شده را مشخص کرد. نتایج بدست‌آمده بیان می‌کنند که با تنظیم پارامترهای الکترومکانیکی می‌توان تا ۶۶ درصد توان ورودی و ۲۷ درصد ولتاژ اعمالی را برداشت کرد. انتخاب پارامتر هندسی مناسب می‌تواند بازده‌های توان و ولتاژهای متصل به الکترودها و سیم پیچ خارجی را به ترتیب به میزان‌های ۱۲۰/۳۱، ۴۹/۰۵ و ۶۰/۹۸ درصد افزایش دهد. به عنوان نتیجه‌گیری نهایی، می‌توان به اثبات مفید بودن استفاده دوگانه (محرک - برداشت‌کننده) از برداشت‌کننده‌های انرژی پیشنهادی اشاره کرد.